KSCE Journal of Civil Engineering (2016) 20(4):1314-1322

DOI 10.1007/s12205-015-0043-7

Geotechnical Engineering

pISSN 1226-7988, eISSN 1976-3808
www.springer.com/12205

Assessment of Concrete Maturity and Overturning Mechanism of Primary Diaphragm Walls in Very Soft Clay during Cold Winter

James C. Ni*, Wen-Chieh Cheng, and Louis Ge*****

Received January 13, 2015/Accepted April 10, 2015/Published Online August 21, 2015

Abstract

Many underground excavation failures are caused by severe water inflow due to the piping through the opening in the diaphragm wall. The opening can be created by slurry pocket or air pocket during concrete placement by tremie method. This type of defect in diaphragm wall can be detected by sonic logging to show the condition of trench wall and by measuring actual concrete dosage during placing. The same detecting method can be used in two very rare case histories where just-completed primary panels in very soft and thick clay deposit were overturned from the adjacent tremie concreting secondary panel during cold winter. The abnormal increasing concrete dosage and the smooth trench wall profile of secondary panel from sonic logging identify the occurrence of this incident. The causes to trigger this incident include (1) panel size, (2) weather condition, (3) tremie concreting speed of secondary panel, (4) initial and final setting times of concrete in trench, (5) roughness of trench wall, etc. Since the temperature for the two case histories is very low during tremie concreting, the initial setting time of concrete in secondary panel, given by equivalent age maturity function, is much longer than the time to place the concrete in secondary panel. To clarify the failure mechanism, the force-equilibrium analysis of inclined primary panel is conducted taking into account the driving force induced by the concrete pressure in the unset secondary panel and the resistant force given by the adhesion between inclined primary panel and soft clayey soil. It can be concluded from this investigation that the concrete in the secondary panel due to lower concrete curing temperature still remains unset or in plastic form and this will generate much larger driving force to push the adjacent just-completed primary panel to tilt. The measures to prevent similar incidents from happening are also suggested in this paper.

Keywords: *concrete maturity, primary diaphragm wall panel, setting time, tremie concreting*

1. Introduction

For a diaphragm wall construction, primary and secondary panels are constructed in alternating order (or pilgrim). Primary panels are constructed after a guide wall is prepared. Each secondary panel is then placed in between two primary panels and closing the gaps. End plates are used to form joints in connecting primary and secondary panels. They make the diaphragm wall system watertight and are able to transfer external forces like bending and shear forces during basement excavation. End plates and nylon sheets bound along both sides of end plate are together used to form a blocking screen to keep the tremie concrete from detouring into the evacuated slurry trench (Ou, 2006).

The tremie method is to be used for concrete placement, during which concrete displaces the bentonite slurry from bottom of trench to prevent concrete from mixing with bentonite slurry. As the concrete continues to rise in the trench, the tremie pipe should be shortened accordingly and the embedded length of tremie pipes in concrete should be maintained below the concrete surface at least 2 meters to prevent cold joints from forming. Therefore, the concrete of first pouring can be ultimately found at the top of the panel and any possible impurities that are picked up from contact with bentonite slurry can be cleaned without difficulty. If the trench wall profile from sonic logging displays the necking nature, the actual concrete dosage should be less than the designed dosage. However, the under dose can be either caused by voids in diaphragm wall or necking of trench wall or both. On the other hand, the over dose due to trench wall collapse could also be occurred together with the necking phenomenon (Ni and Cheng, 2012). Any abnormal conditions can be diagnosed in the first place by comparing the actual concrete dosage to the designed dosage along with the condition of trench wall profile from sonic logging.

The practice mentioned above can produce good quality of diaphragm wall in general. However, there are two very rare

*Professor, Dept. of Civil Engineering, National Taipei University of Technology, Taipei 10608, Taiwan (E-mail: ckni@ntut.edu.tw)
**Formerly Research Associate, College of Engineering, National Taipei University of Technology, Taipei 10608, Taiwan (Corresponding Author, E-mail: s2428030@gmail.com)
***Professor, Dept. of Civil Engineering, National Taiwan University, Taipei 10617, Taiwan (E-mail: louisge@ntu.edu.tw)

failure cases where just-finished adjacent primary panels are tilted away from the concreting secondary panel. There are three common features in these two failure cases. Firstly, the temperature during diaphragm wall construction was very low, down to 14°C. Secondly, the subsoil is very soft and thick clay deposit, with undrained shear strength less than 20 kPa. Lastly, the tremie concreting speed, hitting a rise of 17 m per hour, was unusually fast. The objectives of this paper are: (i) to clarify the failure mechanism of primary diaphragm walls in very soft clay during cold winter and (ii) to provide a checklist after this investigation to prevent similar incidents from happening again.

2. Case I

2.1 Site Characterization

Plan view of the alternatively constructed 1-m thick, 41.2-m deep primary and secondary panels is given in Fig. 1(a). The daytime temperature was around 14°C and was even lower in the night. During concrete pouring, the concrete level following each pouring was recorded and compared with the designed concrete dosage as shown in Fig. 2. The smooth trench wall profile detected from the sonic logging of the concreting secondary panel shown in Fig. 2 rules out the possibility of over dose of concrete. Before the concrete level rises to 10 m below

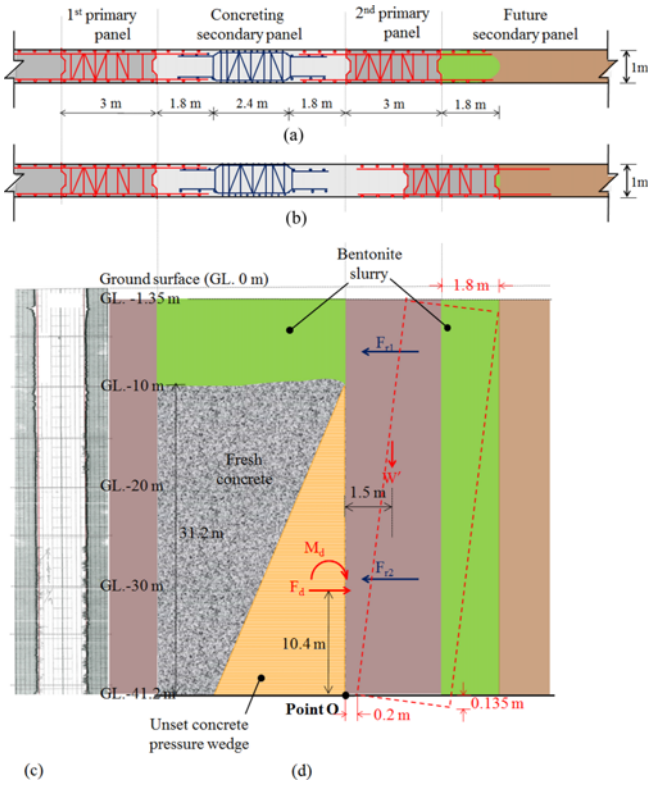

Fig. 1. Force-equilibrium Analysis and Trench Wall Profile from Sonic Logging for Case I (after Ni and Cheng, 2014): (a) Before 2nd Primary Panel Overturning, (b) After 2nd Primary Panel Overturning, (c) Sonic Logging of 2nd Primary Panel, (d) Force-equilibrium Analysis

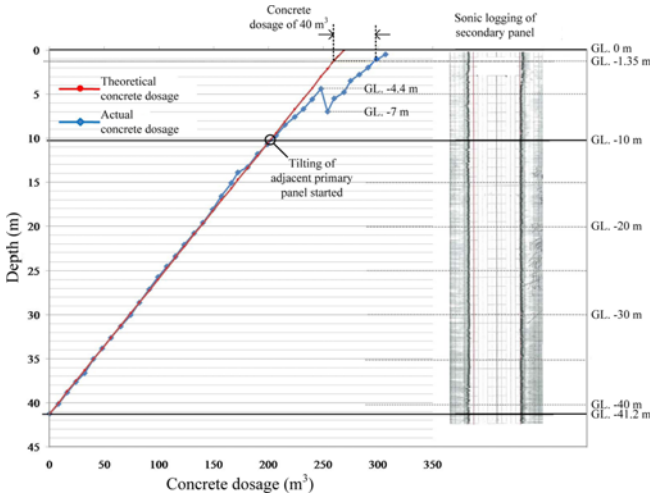

Fig. 2. Actual and Theoretical Concrete Dosages and Trench Wall Profile from Sonic Logging for Case I (after Ni and Cheng, 2014)

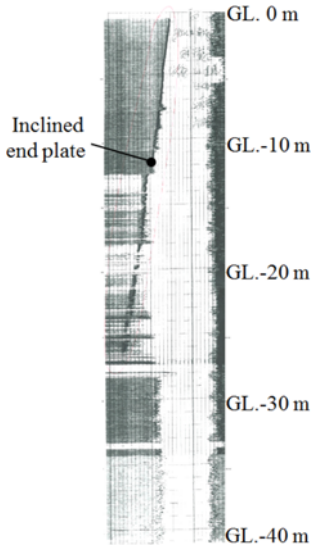

Fig. 3. Sonic Logging of End Plate at Right Hand Side of 2nd Primary Panel (after Ni and Cheng, 2014)

the ground surface, the actual concrete dosage matches reasonably well with the designed dosage. However, after the concrete level exceeds 10 m below the surface the actual concrete dosage begins exceeding the designed dosage, at which time the adjacent primary panel starts to tilt. The sonic logging after excavation of the successive secondary panel supports this point of view (Fig. 3). The increase of 40 m^3 in concrete dosage is almost identical to the volume of trapezoid region created by moving a 39.85-m tall primary panel sideways 1.8 m at top and 0.2 m at bottom, as shown in Fig. 1(d). Some serious construction issues related to this event are highlighted as follows. Firstly, the steel cage overlapping between the just-finished primary panel and the concreting secondary panel may not be sufficient (Fig. 1(b)). Secondly, the construction of the successive secondary panel and fulfilling a required overlapping

Table 1. Physical and Mechanical Properties of Subsoil for Case I (after Ni and Cheng, 2014)

Depth (m)	Blow count N	Soil Type	Water Content ω (%)	Unit Weight γ_t (kN/m^3)	Liquid limit LL (%)	Plasticity index PI (%)	Sand (%)	Silt (%)	Clay (%)	Uniaxial compressive strength q_u (kN/m^2)	S_u, from SUU (kN/m^2)	Optimal S_u (kN/m^2)
1	2	CL	35	18.15	49	24	10	49	41			7.053
2	2	CL	37	18.05	51	26	10	58	32			7.877
3	2	CL	37	17.46	51	26	10	58	32	NDA		8.554
4	2	CL	40	17.36	43	21	5	73	22			8.476
5	2	CL	36	17.36	43	21	4	64	32			9.457
6	1	CL	36	17.27	43	21	4	64	32	20.6		7.524
7	2	CL	32	17.66	38	16	6	69	25			11.134
8	2	CL	35	17.66	35	13	3	58	39	NDA		10.644
9	2	CL	35	15.79	35	13	3	58	39		NDA	10.006
10	2	CL	25	15.79	32	12	4	73	23	50.0		14.048
11	2	CL	28	18.34	31	12	4	76	20			13.930
12	2	CL	28	18.54	31	12	4	76	20	NDA		14.843
13	3	CL	33	18.54	35	12	1	63	36			18.149
14	3	CL	35	18.25	35	11	1	47	52			17.658
15	5	CL	35	18.25	35	11	1	47	52	66.7		26.095
16	5	CL	35	18.25	36	15	0	37	63			25.388
17	5	CL	33	17.27	38	17	1	54	45			26.183
18	4	CL	33	17.27	38	17	1	54	45	NDA	31.4	25.329
19	5	CL	30	16.48	39	16	2	50	48			29.116
20	5	CL	32	16.48	39	18	1	57	42			27.615
21	5	CL	32	18.05	39	18	1	57	42		NDA	31.264
22	6	CL	33	17.76	37	18	1	61	38	108.9		35.385
23	6	CL	36	18.25	37	16	0	55	45			32.814
24	7	CL	36	18.25	37	16	0	55	45		54.9	39.260
25	8	CL	30	18.84	36	15	2	66	32		NDA	45.489
26	8	CL	35	18.84	38	14	0	48	52	NDA		43.576
27	7	CL	35	17.95	38	14	0	48	52		52.0	41.908
28	10	CL	26	19.13	36	18	3	65	32		58.9	61.774
29	10	CL	29	19.13	34	14	1	70	29		NDA	54.916
30	7	CL	29	18.25	34	14	1	70	29	127.5	37.3	49.236
31	8	CL	34	18.25	35	9	0	50	50	NDA		44.488
32	8	ML	34	18.34		NP	2	70	28		NDA	24.525
33	12	ML	33	18.34	NDA	NP	2	70	28	94.2		39.142
34	12	ML	32	18.25		NP	7	76	17	64.7	49.1	40.810
35	10	CL	32	18.25	41	17	1	55	44	n/a		61.607
36	13	CL	32	18.64	41	17	1	55	44	143.2		76.793
37	13	CL	24	19.03	28	10	38	53	9			71.564
38	13	CL	24	19.91	26	10	20	61	19		NDA	70.760
39	12	CL	24	19.91	26	10	20	61	19	NDA		68.503
40	12	ML	25	18.84	NDA	NP	39	49	12			36.788
41	11	ML	30	18.93		NP	5	71	24			33.717

NDA = No Data Available

of steel cages with the primary panel are not likely to be conducted (Fig. 1(b)).

2.2 Subsoil Conditions

The borehole logging and properties of soil on site are given in Table 1, by which the estimate of the undrained shear strength, S_u, can be conducted using the following four methods. Firstly, the blow count N value can be converted to S_u using Eq. (1) (Japan Road Association, 1977). Secondly, the moisture content with the Atterberg limits can also be used to provide the estimate of S_u by using Eq. (2) (Bjerrum and Simons, 1960). Thirdly, S_u can be estimated using the unconfined compressive strength q_u (Eq. (3)). Lastly, Unconsolidated Undrained (UU) triaxial test is the simplest and quick way to determine S_u of undisturbed and

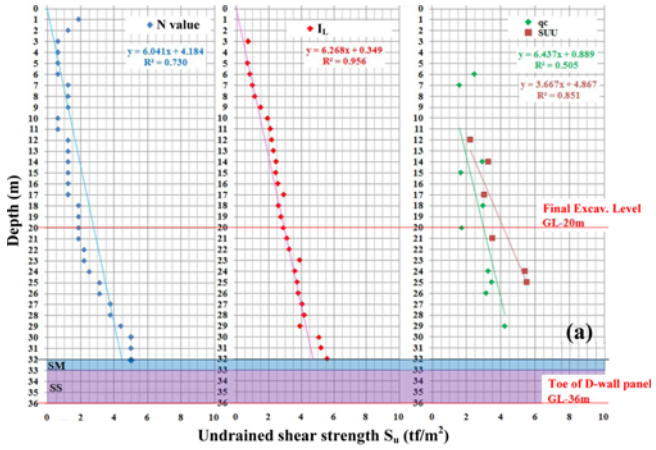

(b)

Objective function f (1)	f1 = N value / 1.6 (Eq. 1)	f2 = 0.18 × σ_i' × $(I_L)^{0.5}$ (Eq. 2)	f3 = q_u / 2 (Eq. 3)	f4 = S_u from SUU test
Weighting factor (2)	0.25	0.6	0.05	0.1
(1) × (2) =	0.25 × f1	0.6 × f2	0.05 × f3	0.1 × f4
Optimized estimate of S_u = Σ (1) × (2)	0.25 × f1 + 0.6 × f2 + 0.05 × f3 + 0.1 × f4			

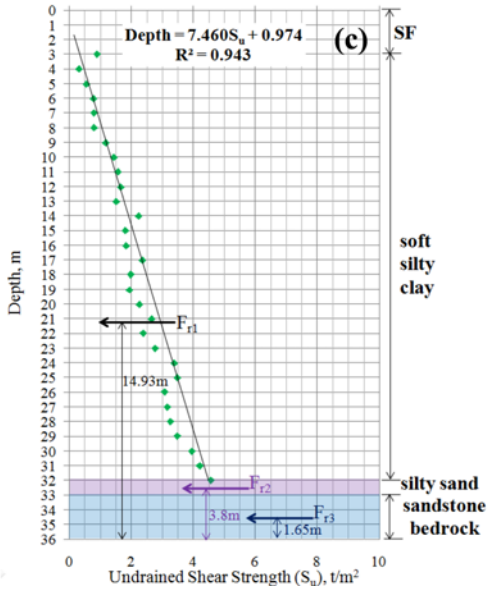

Fig. 4. Optimal Undrained Shear Strength Profile for Case I (after Ni and Cheng, 2014)

saturated soil samples. In this study, an optimization method suggested by Marler and Arora (2004) is utilized to conduct the estimate of the optimal undrained shear strengths taking into account different weighting factors, depending on the R-square of regression analysis in raw data quality, onto S_u (Eq. (4)). A minor adjustment of the weighting factor has been made to consider the nature of slightly over-consolidated surface soil despite the poorer fit of the blow count data than the liquidity index I_L data (Fig. 4(b)). Consequently, the optimal undrained shear strength profile can be obtained, as shown in Fig. 4(c). The friction force between concrete panel and in-situ soil is controlled by the S_u value of clayey soils and counterbalances the driving force resulting from concrete pressure of the concreting diaphragm wall panel which in turn is a function of time of setting.

$$S_u(\text{t/m}^2) = \text{N value} / 1.6 \quad (1)$$

$$S_u(\text{t/m}^2) = 0.18 \times \sigma_i' \times (I_L)^{0.5} \quad (2)$$

where I_L is liquidity index

$$S_u = q_u / 2 \quad (3)$$

$$S_u = 0.5 \times \text{N value} / 1.6 + 0.4 \times 0.18 \times \sigma_i' \times (I_L)^{0.5} + 0.05 \times q_u / 2 + 0.05 \times S_u \text{ (from SUU)} \quad (4)$$

2.3 Time of setting

Concrete pressure during its tremie concreting of the secondary panel is a function of time of setting and this pressure would be larger when concrete remains unset due to lower concrete curing temperature and fast concrete placement, thereby resulting in the primary panel tilting. The initial setting time under cold weather conditions is longer than that under normal temperatures (Carino and Lew, 2001; Brooks *et al.*, 2007). Therefore, it is important to know setting times of concrete samples cured with fluctuating temperatures using the equivalent age maturity technique, even if concrete mixtures are made with different water-to-cement ratios and supplementary cementing materials (Brooks *et al.*, 2007; Wade *et al.*, 2010).

With this maturity technique, initial and final setting times in the ranges of usual practice for which the most commonly used mixture-specific setting-maturity relationship and activation energy are introduced can be estimated. In general, the time of setting due to the use of fly ash can be increased at different rates relating to the type of fly ash. The use of slag seems to have small influence on setting times. The equivalent age maturity function outlined in ASTM C 1074 (2011) is given in Eq. (5) which has been accepted as the most accurate maturity formula.

$$t_e = \sum_0^t \exp\left[-\frac{E}{R}\left(\frac{1}{273+T_c}-\frac{1}{273+T_r}\right)\right]\times\Delta t \quad (5)$$

Where E = activation energy(J/mol)
R = universal gas constant (8.314 J/mol K)
T_c = Average concrete temperature during interval Δt (°C)
t_e = Equivalent age at reference curing temperature (hr)
T_r = Initial datum temperature (°C)
Δt = A time interval (hr)

Hansen and Pedersen (1977) proposed the activation energy formula, relating the activation energy to the concrete temperature (T_c) as shown in Eq. (6). The equivalent age maturity after incorporating Hansen and Pedersen (1977) can produce the best-fit results of compressive strengths (t_e < 100h) at uniform curing temperatures ranging from -10 to 80°C.

$$E(T_c) = 33{,}500 \text{ J/mol for } T_c \geq 20°\text{C} \quad (6a)$$

Table 2. Concrete Mixture Properties for Case I (after Ni and Cheng, 2014)

Water-to-Cementitious Materials Ratio	0.47
Water (kg/m^3)	188
Cementitious Materials (kg/m^3)	400
Type I Cement (kg/m^3)	320
Aggregate (kg/m^3)	1822.1
Slag (kg/m^3)	40
Fly Ash (kg/m^3)	40
Concrete Strength (kg/cm^2)	280

$$E(T_c) = 33{,}500 + 1{,}470 \times (20 - T_c)\ \text{J/mol for } T_c < 20^{\circ}\text{C} \quad (6b)$$

During tremie concreting of the secondary panel, the temperature T_c was as low as 14ºC. By Eq. (6), the activation energy can be estimated as 42320 J/mol which is within the range of 40,000-45,000 J/mol recommended by ASTM C 1074 (2011) for strength estimations for which Type 1 Portland cement with no admixtures is used.

Since the concrete mixture (Table 2) adopted on this site is very similar to that adopted by Wade *et al.* (2010). The initial setting time is about 4.2 hours if concrete is cured at constant temperature of 23ºC (Wade *et al*., 2010). However, by Eq. (5), the initial setting time due to this lower concrete curing temperature of 14ºC is longer; that is, 7.2 hours. As the tremie concreting speed for this secondary panel was as fast as 10 m/hr, it takes only 3.1 hours for concrete surface rising from bottom (GL.-41.2 m) to 10 m below the ground surface, which is much shorter than the initial setting time of 7.2 hours, indicating that the concrete in the secondary panel still remains unset or in plastic form and this will generate much larger driving force to push the adjacent just-finished primary panel to tilt.

2.4 Equilibrium Conditions

The diagram of the driving forces and resistant forces acting on the tilted primary panel are given in Fig. 1(d). The overturning point, Point O, is at the lower left corner according to the observations on site over this incident. The driving forces include two components, the unset concrete pressure, F_d = 11446.4 kN (Eq. (7)) and the self-weight minus buoyant force of primary panel, W' = 1687.6 kN (Eq. 8). It can be seen from Fig. 4(c) that the horizontal resistant force resulted from the adhesion between primary panel and soft clay is derived from the S_u value in two parts, F_{r1} and F_{r2} (Eqs. (9) and (10)). Since the total horizontal resistant force of 9388.4 kN plus base friction is a bit less than the driving force of 11446.4 kN, the primary panel is thus horizontally moved by 0.2 m as shown in Fig. 1(d). By Eq. (11), the safety factor against overturning is calculated as 0.99, indicating that the primary panel starts to tilt when the concrete surface rises to 10 m below the surface. Because on-site crew are kept in the dark, tremie concreting still carries out until overturning accompanied by the sudden drop of concrete surface from 4.4 to 7 m below the surface occurs (Fig. 2).

$$F_d = \gamma_c \times t \times k_h \times \int_0^d z\,dz \quad (7)$$

where t and k_h are panel thickness and lateral earth pressure coefficient, respectively,

$$W' = (\gamma_c - \gamma_w) \times V_{panel} \quad (8)$$

$$F_{r1} = [(0.5+1.5) \times 9.65/2] \times 3 \times 2 \times 9.8 = 568.4\ \text{kN} \quad (9)$$

$$F_{r2} = [(0.5+8.5) \times 30/2] \times 3 \times 2 \times 9.8 = 8820\ \text{kN} \quad (10)$$

$$FOS = M_r / M_d \quad (11)$$

where

$M_d = (11446.4 \times 10.4 + 1687.6 \times 1.5) = 121574$ kN-m

$M_r = (568.4 \times 34.22 + 8820 \times 11.5) = 120880.6$ kN-m

3. Case II

3.1 Site Characterization

Figure 5(a) shows the diagram of 1.2-meter thick and 36.3-

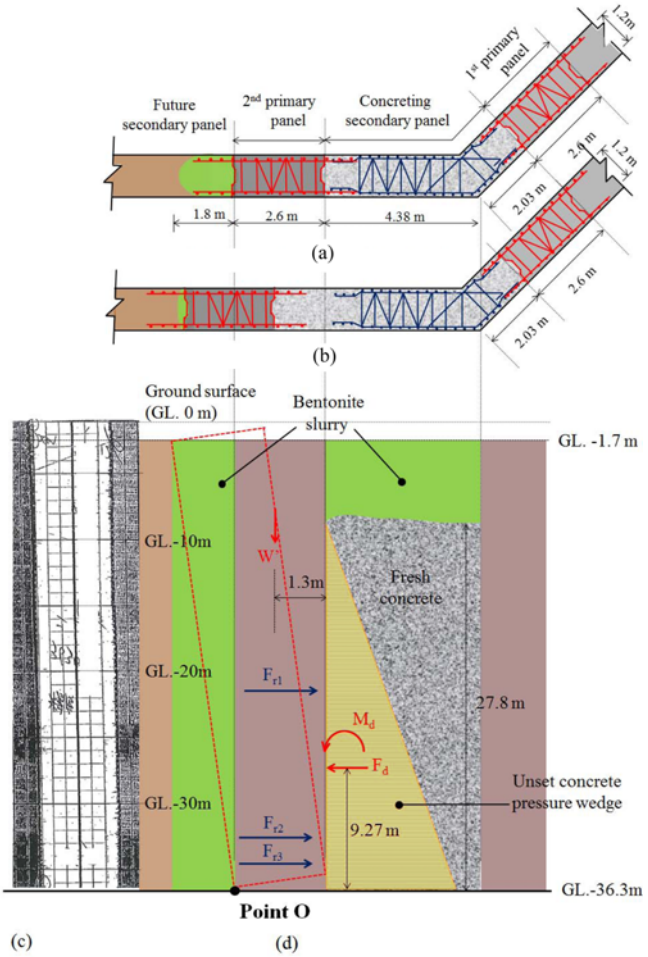

Fig. 5. Force-equilibrium Analysis and Trench Wall Profile from Sonic Logging for Case II: (a) Before 2nd Primary Panel Overturning, (b) After 2nd Primary Panel Overturning, (c) Sonic Logging of 2nd Primary Panel, (d) Force-equilibrum Analysis

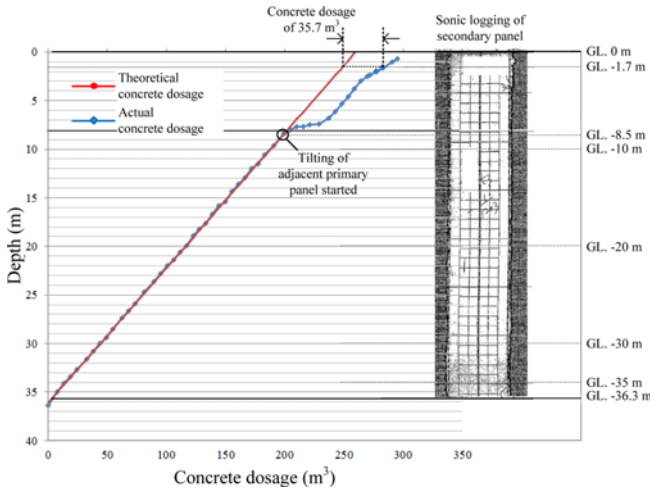

Fig. 6. Actual and Theoretical Concrete Dosages and Trench Wall Profile from Sonic Logging for Case II

meter deep primary and secondary diaphragm wall panels. A faster speed of 17 meters per hour was used for concreting this secondary panel. The daytime temperature was about 15°C and even colder into the night. The sonic logging of the secondary panel in Fig. 6 shows the ideal trench wall profile. Thus, the actual concrete take should be similar to the theoretical value. This is observed until concrete surface rises to GL.-8.5 m, and then the abnormal increase of concrete take over theoretical value occurs. It is believed that this is the moment the panel starts to incline.

3.2 Subsoil Conditions

This site is covered with a 2-meter backfilled material underlain by a very thick and soft silty clay deposit to GL.-32 m, and then followed by a 1-meter silty sand thin layer and sandstone bedrock. The borehole logging and properties of soil on site are given in Table 3. The same optimization method adopted in the previous case history is utilized to estimate the optimal undrained shear strengths as shown in Eq. (12). Consequently, the optimal undrained shear strength profile can be obtained, as shown in Fig. 7(c).

$$S_u = 0.25 \times \text{N value} / 1.6 + 0.6 \times 0.18 \times \sigma_i' \times (I_L)^{0.5} + 0.05 \times q_u / 2 + 0.1 \times S_u \text{ (from SUU)} \quad (12)$$

3.3 Time of Setting

Since the concrete mixture (Table 4) adopted is similar to previous case history, the same procedure as in previous case history can be utilized to estimate the initial setting time. The initial setting time of concrete due to this lower concrete curing temperature of 15°C is estimated as 6.7 hours. According to the reported tremie concreting speed as fast as 17 m/hr, it takes only 1.6 hours for concrete surface rising from trench bottom to 8.5 m below the surface. This is much shorter than the initial setting time of 6.7 hours, revealing that the concrete in the concreting

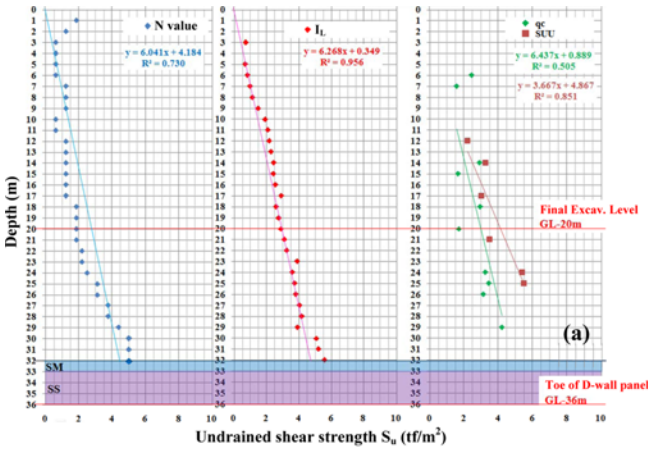

(b)

Objective function f (1)	f1 = N value / 1.6 (Eq. 1)	f2 = 0.18 × σ_i' × $(I_L)^{0.5}$ (Eq. 2)	f3 = q_u / 2 (Eq. 3)	f4 = S_u from SUU test
Weighting factor (2)	0.25	0.6	0.05	0.1
(1) × (2) =	0.25 × f1	0.6 × f2	0.05 × f3	0.1 × f4
Optimized estimate of S_u = Σ (1) × (2)	0.25 × f1 + 0.6 × f2 + 0.05 × f3 + 0.1 × f4			

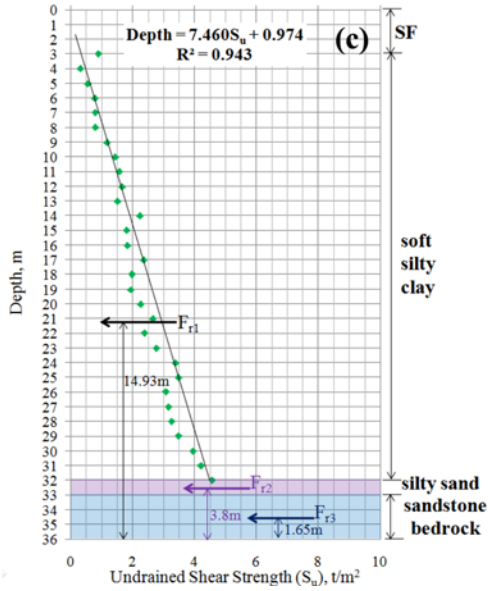

Fig. 7. Optimal Undrained Shear Strength Profile for Case II

closing panel still remains unset or in plastic form and this will result in much larger driving force (Eq. (13)) to overturn the adjacent primary panel.

$$F_d = \gamma_c \times t \times k_h \times \int_0^d z\,dz = (2.4 \times 1.2 \times 1) \times \int_0^{27.8} z\,dz \times 9.8 = 10906.2 \text{ kN} \quad (13)$$

3.4 Equilibrium Conditions

Figure 5(d) is the overturned primary panel on which driving forces and resistant forces apply. The driving forces are the unset concrete pressure, F_d, from Eq. (13) and the self-weight minus buoyant force of primary panel, W', from Eq. (14). The horizontal

Table 3. Physical and Mechanical Properties of Subsoil for Case II

Depth (m)	Blow count N	Soil Type	Water Content ω (%)	Unit Weight γ_t (kN/m^3)	Liquid limit LL (%)	Plasticity index PI (%)	Gravel (%)	Sand (%)	Silt (%)	Clay (%)	Uniaxial compressive strength q_u (kN/m^2)	S_u, from SUU (kN/m^2)	Optimal S_u (kN/m^2)
1	NDA	SF	28	21.68	NDA	NDA	0	89	11	0			
2		SF	27	21.68			3	14	59	24			
3	3	CL	29	18.93	38	18	3	14	59	24	NDA		9.692
4	2	CL	36	18.05	37	16	0	29	53	18			3.679
5	1	CL	42	17.46	41	16	0	1	73	26			5.847
6	1	CL	42	17.46	41	16	0	1	73	26	48.1	NDA	6.641
7	1	CL	41	17.66	39	16	0	2	69	29	30.4		7.426
8	1	CL	41	17.66	39	16	0	2	74	24			8.231
9	2	CL	34	18.25	35	14	0	2	74	24			12.184
10	2	CL	32	18.74	36	16	0	3	66	31	NDA		14.754
11	2	CL	32	18.74	36	16	0	3	71	26			15.892
12	1	CL	33	18.64	35	11	0	3	71	26		21.6	16.648
13	1	CL	31	18.54	33	13	0	2	70	28		NDA	15.156
14	2	CL	31	18.54	33	13	0	1	66	33	56.9	31.9	21.209
15	2	CL	38	17.95	40	18	0	1	66	33	32.4	NDA	17.668
16	2	CL	38	17.95	40	18	0	0	69	30	NDA		18.600
17	2	CL	37	17.85	42	20	0	1	64	35		29.4	23.672
18	2	CL	40	17.56	40	20	0	1	64	35	57.9		18.737
19	2	CL	41	17.76	40	21	0	1	61	38	n/a	NDA	19.600
20	3	CL	41	17.76	40	21	0	1	65	34	33.4		22.279
21	3	CL	43	17.17	46	21	0	1	65	34		34.3	26.968
22	3	CL	43	17.17	46	21	0	1	66	33	NDA	NDA	24.397
23	3	CL	38	17.66	43	19	0	1	70	29			28.223
24	3.5	CL	39	17.66	40	17	0	1	70	29	63.8	53.0	32.697
25	3.5	CL	39	17.66	40	17	0	2	68	30	67.7	54.0	33.668
26	4	CL	40	17.36	42	19	0	1	63	36	60.8		29.773
27	5	CL	39	17.66	40	19	0	1	63	36	NDA		32.707
28	5	CL	39	17.66	40	19	0	1	66	33			33.570
29	6	CL	42	17.36	41	18	0	3	70	27	82.4	NDA	34.060
30	6	CL	36	18.25	39	20	0	3	70	27			38.720
31	7	CL	36	18.25	39	20	0	2	68	30	NDA		40.682
32	8	SM	35	17.85	40	18	0	85	15	0			44.488
33	Sandstone Bedrock (RQD = 50)											7769.5	
34	Sandstone Bedrock (RQD = 80)												
35	Sandstone Bedrock (RQD = 60)												
36	Sandstone Bedrock (RQD = 50)												

NDA = No Data Available

Table 4. Concrete Mixture Properties for Case II

Water-to-Cementitious Materials Ratio	0.46
Water (kg/m^3)	185
Cementitious Materials (kg/m^3)	400
Type I Cement (kg/m^3)	300
Aggregate (kg/m^3)	1830.1
Slag (kg/m^3)	50
Fly Ash (kg/m^3)	50
Concrete Strength (kg/cm^2)	280

resistance forces between panel concrete and three types of in-situ soils are F_{r1}, F_{r2} and F_{r3} (Eqs. (15), (16) and (18)). F_{r1} is the product of contact area and optimal undrained shear strength of soft clay from Fig. 7. F_{r2} is the product of normal force and friction coefficient between silty sand and concrete. As the diaphragm wall panel is embedded into bedrock three meters, the friction between concrete panel and sandstone should be controlled by the weaker concrete because of less curing time. This concrete is cured only 56 hours before the secondary primary panel started to tilt. Nurse-Saul maturity function (Eq. (17)) is used to estimate the Maturity Index with a datum temperature of 11ºC suggested by Carino and Tank (1992) as shown in Fig. 8. By using a strength-maturity relation (Nixon *et al.*, 2008), with M = 369ºC · hours, the concrete strength of 3430

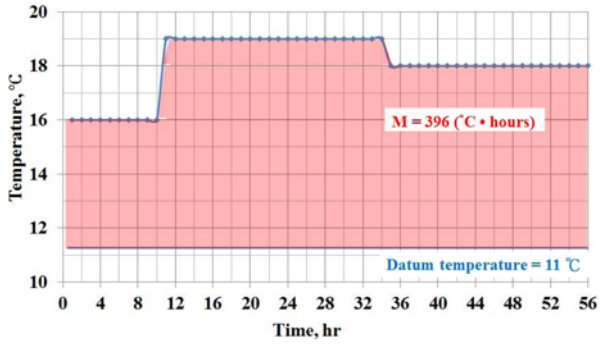

Fig. 8. Diagram of Concrete Curing Temperature Over Time

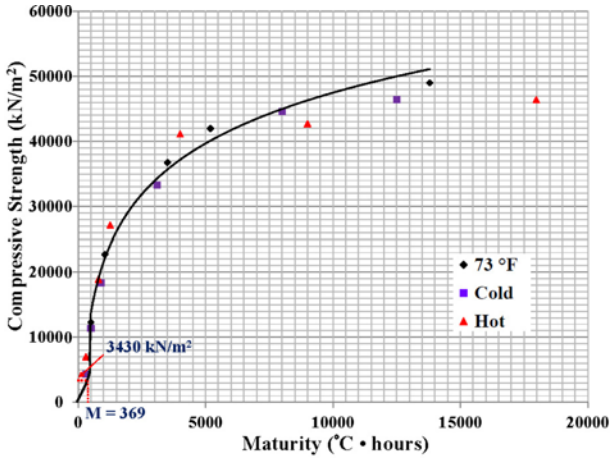

Fig. 9. Relationship between Compressive Strength and Maturity (after Nixon *et al.*, 2008)

kPa (Fig. 9) is estimated and this is much smaller than sandstone (Table 3). As concrete strength is not sensitive to the confining pressure, the shear strength is close to half of compressive strength. Then by Eq. (18), F_{r3}, friction between sandstone bedrock and panel concrete cured for 56 hours, can be evaluated, which is much larger than the driving force. This indicates that the primary panel cannot move horizontally. However, the safety factor against overturning is 1.05 (Eq. (19)) less than 1.5, and this explains the overturning mechanism.

$$W' = (\gamma_c - \gamma_w) \times V_{panel} = (2.4 - 1) \times (2.6 \times 36.3 \times 1.2) \times 9.8 = 1553.8 \text{ kN} \quad (14)$$

$$F_{r1} = [(0.2 + 4.5) \times 30.6 / 2] \times 2 \times 2.6 \times 9.8 = 3664.5 \text{ kN} \quad (15)$$

$$F_{r2} = 2 \times N \times \tan\phi = 2 \times 32.5 \times \tan 32° = 398 \text{ kN} \quad (16)$$

where

$$N = \gamma \times k_0 \times L \times \int_0^d z\,dz = 0.82 \times 0.47 \times 2.6 \times \int_{32}^{33} z\,dz \times 9.8 = 318.5 \text{ kN}$$

$$M = (\sum_0^t)(T - T_0) \times \Delta t \quad (17)$$

$$F_{r3} = (S_u \times H) \times (2L) = (1715 \times 3.3) \times (2 \times 2.6) = 29429.4 \text{ kN} \quad (18)$$

$$FOS = M_r / M_d = 106801.8 / 101100.5 = 1.05 \quad (19)$$

where

$M_d = 10906.2 \times 9.27 = 101100.5$ kN-m

$M_r = (F_{r1} \times 14.93 + F_{r2} \times 3.8 + F_{r3} \times 1.65) + (W' \times 1.3)$
$= 106801.8$ kN-m

4. Conclusions

Two very rare failure case histories are presented in this paper. Any abnormal conditions can be diagnosed in the first place by comparing the actual dosage to the designed dosage along with the trench wall profile from sonic logging. The failure mechanism of overturning primary panel is justified by the force-equilibrium analysis and the initial setting time estimated from the equivalent age maturity function. The following conclusions can be drawn:

1. This incident can be diagnosed in the first place through the abnormal increasing concrete dosage during tremie concreting and the smooth trench wall profile of the concreting secondary panel from the sonic logging.
2. The force-equilibrium analysis and the initial setting time estimated from the equivalent age maturity function indicate that the initial setting time under this lower concrete curing temperature was longer than that under normal temperatures and this unset concrete pressure in the concreting secondary panel would generate larger driving force to push the just-completed adjacent primary panel to tilt. Unusual fast concreting speed and small shear resistance in very soft and thick clayey soil may also be considered as the causes to trigger this incident.
3. With observations from the two very rare failure cases, the equivalent age maturity function can be successfully used for determining the initial and final setting times of concrete in trench under non-isothermal curing temperatures.
4. The suggested quality control of concrete dosage during tremie concreting along with the condition of trench wall profile can be used to detect the possibility of the failure mechanism of overturning primary panel and this can also be used in the early design phase to prevent similar foundation failures from occurring again.

Acknowledgements

The on-site construction information provided by Mr. Chih-Hung Shih, the deputy general manager of Tung Feng Construction Engineering Co., Ltd. as well as the data reduction and drawing by Ms. Hwei-Wen Hwang are sincerely acknowledged. This research would not have been possible without the financial support from the National Science Council of Taiwan under the Contract No. NSC97-2622-E-027-013-CC3.

References

ASTM (2011). "Standard practice for estimating concrete strength by the maturity method." C1074,West Conshohocken, PA, DOI: 10.1520/C1074-11.

Bjerrum, L. and Simons, N. E. (1960). "Comparison of shear strength characteristics of normally consolidated clays." *Research Conference of Shear Strength of Cohesive Soils*, Boulder, Colorado, American Society of Civil Engineers, pp. 711-727.

Brooks, A. G., Schindler, A. K., and Barnes, R. W. (2007). "Maturity method evaluated for various cementitious materials." *Journal of Materials in Civil Engineering*, Vol. 19, No. 12, pp. 1017-1025, DOI: 10.1061/(ASCE)0899-1561(2007)19:12(1017).

Carino, N. J. and Lew, H. S. (2001). "The maturity method:From theory to application." *Proceedings of the 2001 Structures Congress & Exposition*, May 21-23, 2001 Washington, D.C., American Society of Civil Engineers, Reston, Virginia, p. 19, DOI: 10.1061/40558 (2001)17.

Carino, N. J. and Tank, R. C. (1992). "Maturity functions for concrete made with various cements and admixtures." *ACI Materials Journal*, Vol. 89, No. 2, pp. 188-196, DOI: 10.14359/2275.

Freiesleben, H., Hansen, P. F., and Pedersen, E. J. (1977). "Maturity computer for controlled curing and hardening of concrete." *Nordisk Betong*, Vol. 1, No. 19, pp. 21-25.

Japan Road Association (1977). *Guidelines for soft ground measures*, January, 216p (in Japanese).

Marler, R. T., and Arora, J. S. (2004). "Survey ofmulti-objective optimization methods for engineering." *Structuraland Multidisciplinary Optimization*, Vol. 26, No. 6, pp. 369-395, DOI: 10.1007/s00158-003-0368-6.

Ni, J. C. and Cheng, W. C. (2012). "Characterising the failure pattern of a station box of Taipei Rapid Transit System (TRTS) and its rehabilitation." *Tunnelling and Underground Space Technology*, Vol. 32, pp. 260-272, DOI: 10.1016/j.tust.2012.06.010.

Nixon, J. M., Schindler, A. K., Barnes, R. W., and Wade, S. A. (2008). "Evaluation of the maturity method to estimate concrete strength in field applications." *Alabama Department of Transportation*, ALDOT Project 930-590, p. 309.

Ou, C. Y. (2006). *Deep Excavation: Theory and Practice*, Taylor & Francis, London.

Wade, S. A., Nixon, J. M., Schindler, A. K., and Barnes, R. W. (2010). "Effect of temperature on the setting behavior of concrete." *Journal of Materials in Civil Engineering*, Vol. 22, No. 3, pp. 214-222, DOI: 10.1061/(ASCE)0899-1561(2010)22:3(214).